

KfK 5075
Januar 1993

Fully Developed Liquid-Metal Flow in Multiple Rectangular Ducts in a Strong Uniform Magnetic Field

S. Molokov
Institut für Angewandte Thermo- und Fluidodynamik
Projekt Kernfusion

Kernforschungszentrum Karlsruhe

Kernforschungszentrum Karlsruhe
Institut für Angewandte Thermo- und Fluidodynamik
Projekt Kernfusion

KfK 5075

*Fully Developed Liquid-Metal Flow in Multiple Rectangular
Ducts in a Strong Uniform Magnetic Field*

S. Molokov

Kernforschungszentrum Karlsruhe GmbH, Karlsruhe

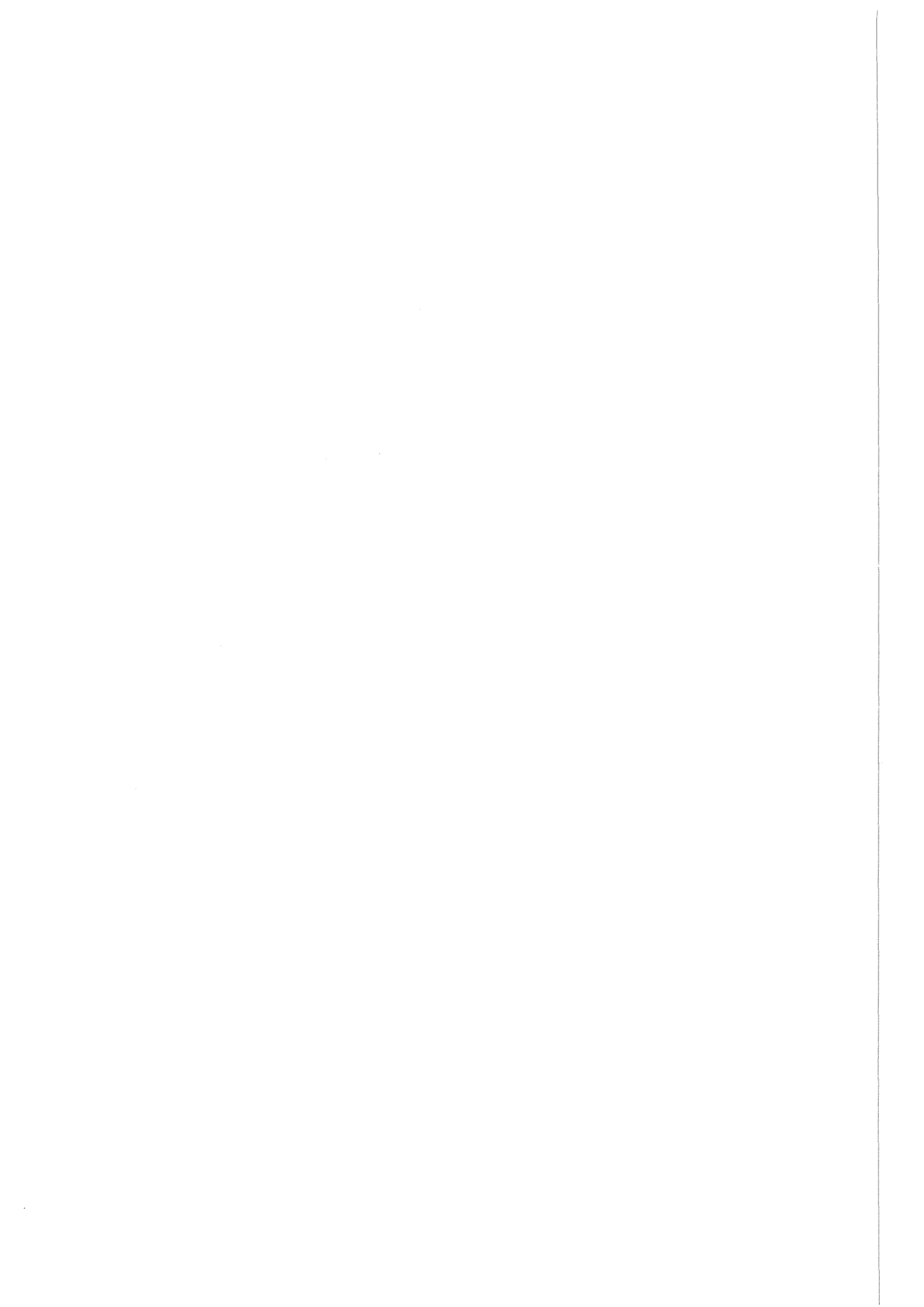
Als Manuskript gedruckt
Für diesen Bericht behalten wir uns alle Rechte vor

Kernforschungszentrum Karlsruhe GmbH
Postfach 3640, 7500 Karlsruhe 1

ISSN 0303-4003

A B S T R A C T

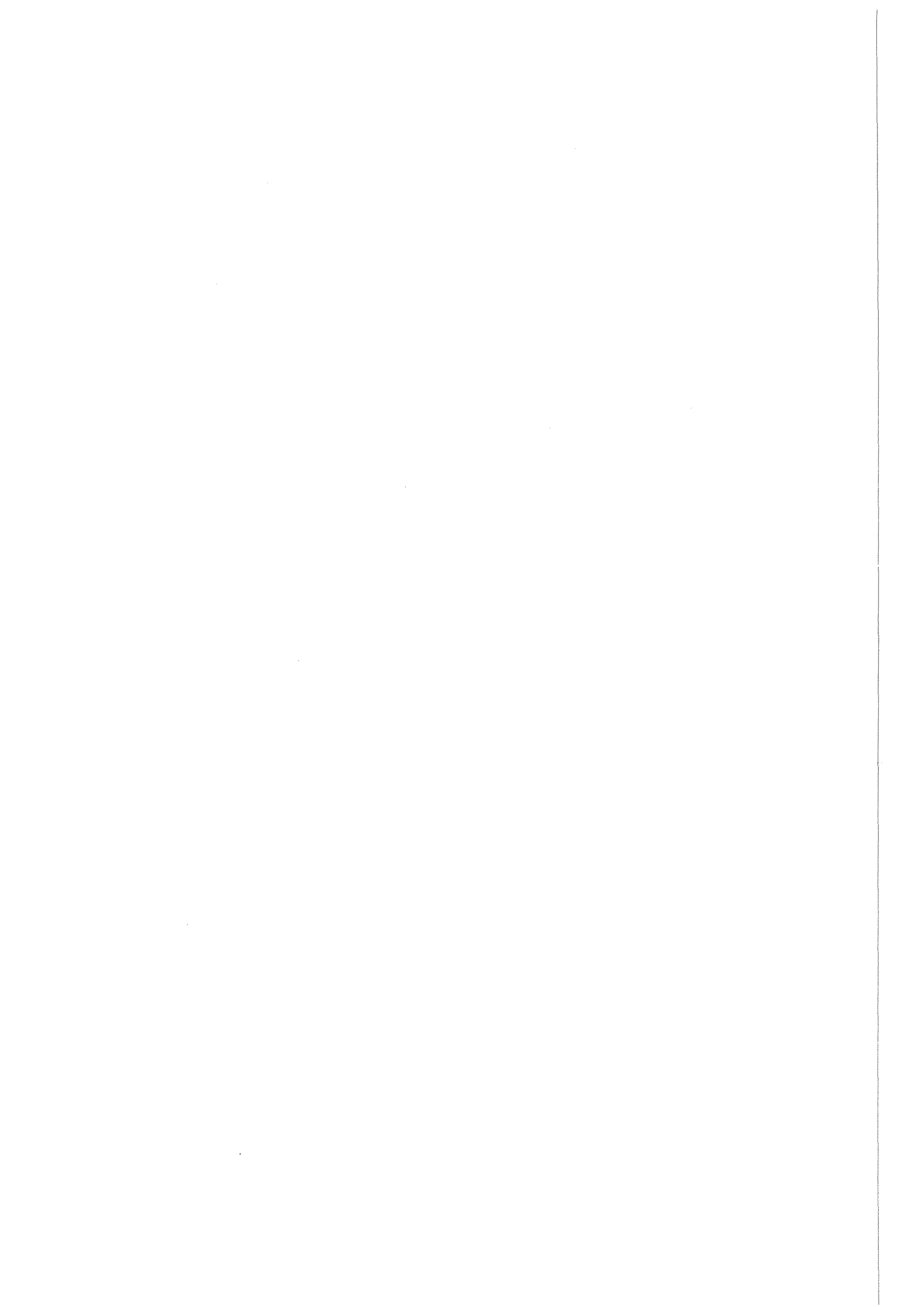
Fully developed liquid-metal flow in a straight rectangular duct with thin conducting walls is investigated. The duct is divided into a number of rectangular channels by electrically conducting dividing walls. A strong uniform magnetic field is applied parallel to duct outside side walls and dividing walls and perpendicular to the top and the bottom walls. The analysis of the flow is performed by means of matched asymptotics at large values of the Hartmann number M . The asymptotic solution obtained is valid for arbitrary wall conductance ratio of the side walls and dividing walls, provided top and bottom walls are much better conductors than the Hartmann layers. The influence of the Hartmann number, wall conductance ratio, number of channels and duct geometry on pressure losses and flow distribution is investigated. If Hartmann number is high, the volume flux is carried by the core, occupying the bulk of the fluid and by thin layers of thickness of the order of $M^{-1/2}$. In some of the layers, however, the flow is reversed. As channel number increases the flow in the channels close to the center becomes of Hartmann type with no jets at the side walls. Estimation of pressure-drop increase in radial ducts of a self-cooled liquid-metal blanket with respect to flow in a single duct with walls of same wall conductance ratio gives the upper limit of 30 per cent.



VOLL ENTWICKELTE FLÜSSIGMETALLSTRÖMUNG IN PARALLELEN KANÄLEN MIT RECHTECKIGEM STRÖMUNGSQUERSCHNITT IN EINEM STARKEN HOMOGENEN MAGNETFELD

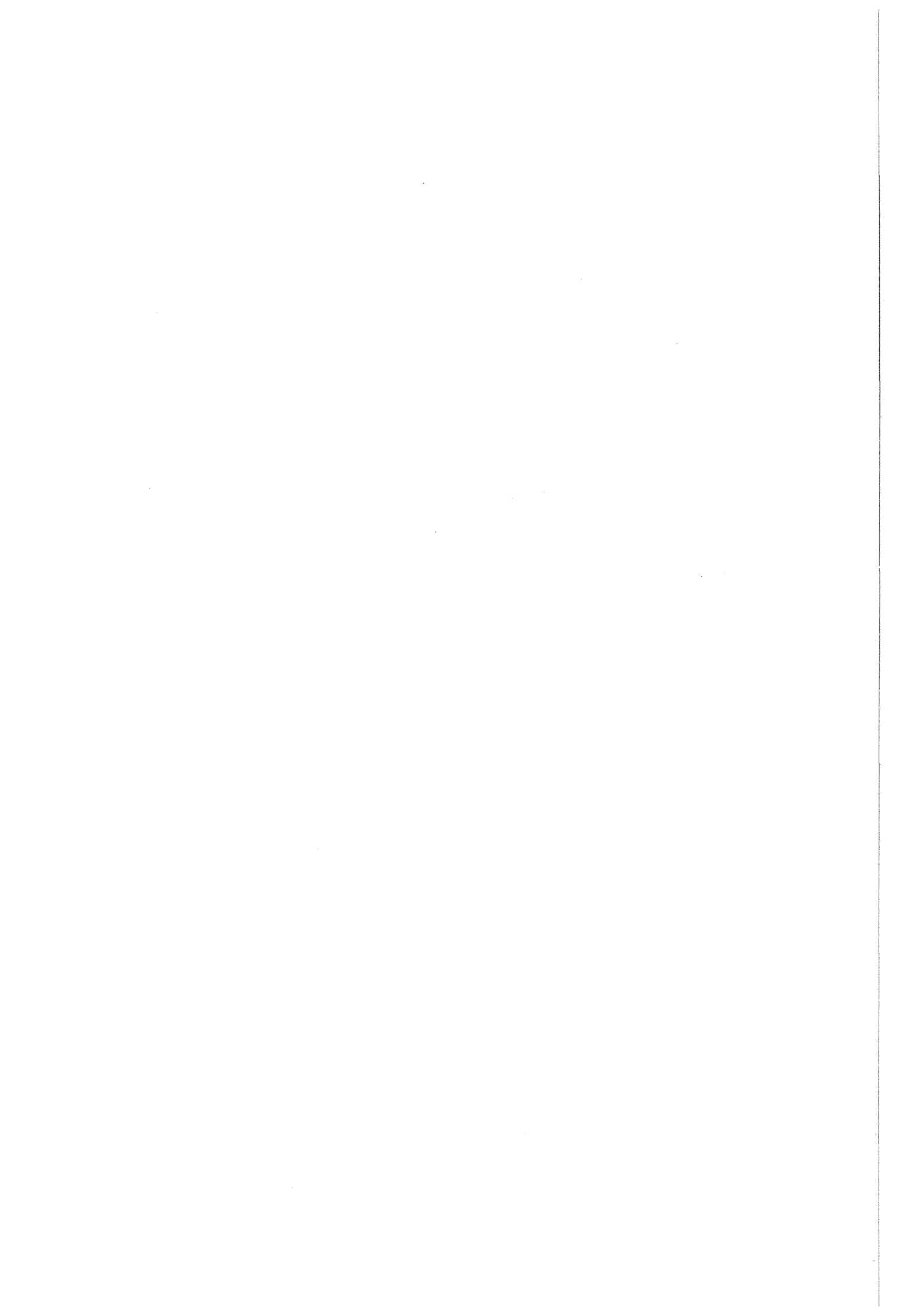
Zusammenfassung

Mehrkanaleffekte in magnetohydrodynamischen (MHD) Flüssigmetallströmungen entstehen bei der Durchströmung von parallelen Kanälen aufgrund der elektrischen Kopplung dieser Kanäle über elektrisch leitende Kanalwände. Diese Effekte werden am Beispiel einer voll eingelaufenen MHD-Strömung in einem Kanal von rechteckförmigem Querschnitt untersucht, der durch dünne elektrisch leitende Zwischenwände in einzelne Unterkanäle aufgeteilt wird. Das angelegte starke Magnetfeld ist parallel zu diesen Zwischenwänden und senkrecht zur oberen und unteren Kanalwand orientiert. Berechnungen für große Hartmann-Zahlen (M) werden mit der Methode der "matched asymptotic expansions" durchgeführt. Die berechnete asymptotische Lösung ist für beliebige Leitfähigkeiten der Zwischenwände und der beiden äußeren Seitenwände gültig, sofern diese besser leitend sind als die Hartmann-Grenzschichten. Untersucht werden die Druckverluste und Geschwindigkeitsverteilungen in Abhängigkeit von der Hartmann-Zahl, der Wandleitfähigkeit und der Anzahl der Teilkanäle sowie ihrer Geometrie. Für große Hartmann-Zahlen fließt der Volumenstrom im wesentlichen im Kern und in dünnen Schichten von der Größenordnung $M^{-1/2}$. In einigen Gebieten ist die Strömungsrichtung umgekehrt. Mit wachsender Kanalanzahl entwickelt sich im mittleren Kanal eine Hartmannströmung ohne Geschwindigkeitsüberhöhungen an den Seitenwänden. Eine Abschätzung der Druckverlustzunahme in den radialen Kanälen eines selbstgekühlten Flüssigmetallblankets bezogen auf die Strömung in einem Einzelkanal mit Wänden gleicher elektrischer Leitfähigkeit, liefert einen oberen Wert von 30 %.



C O N T E N T S

1 Introduction	9
2 Formulation of the problem	14
2.1 Governing equations	15
2.2 Boundary conditions	17
3 Asymptotic solution	21
3.1 The core C and the Hartmann layer H	22
3.2 Side layers SR and SL	23
3.3 Composite solution and flow rates	28
4 Results and discussion	32
4.1 Single channel	-
4.2 Two channels	34
4.3 Three channels and more	35
5 Conclusions	45
References	46
Appendix A: Hartmann layer HS	49



I. INTRODUCTION

In a concept of self-cooled liquid-metal blanket for Tokamaks, the first wall is cooled by liquid metal flowing in radial-toroidal bends [1]. Toroidal ducts are aligned with magnetic field lines to avoid pressure losses caused by strong magnetohydrodynamic interaction. These ducts are fed by the radial ones in which the coolant flows perpendicular to the magnetic field over a short distance. Toroidal ducts are electrically coupled by common electrically conducting dividing walls. This results in the so-called "Multi-Channel Effect" (MCE) caused by leakage currents crossing all channels [2]. MCE is expressed in additional pressure drop with respect to the flow in electrically separated channels and in nonuniform flow distribution among coolant ducts. To suppress leakage currents in radial ducts, i.e. to separate them electrically, Flow Channel Inserts (FCI) are suggested [3]. Without FCI, MCE is present in radial ducts as well.

Contribution to the total pressure drop due to MCE in radial-toroidal bends results from two electric current loops. The first one is two-dimensional in a sense that current flows in planes perpendicular to the main-flow direction. This current is induced in the radial ducts, if FCI are not used; it brings the only contribution to the total MCE far from the junction between ducts in the region of fully developed flow. The second current loop near the junction between radial and toroidal ducts produces three-dimensional pressure drop.

The importance of MCE and its influence on pressure losses has been pointed out first by Madarame, Taghavi & Tillack [2]. They estimated three-dimensional pressure drop in the second wall orifice of BCSS blanket in a multiple duct geometry. The results were obtained by assuming that the top wall was thick, and that the wall conductance ratio c of the thin side walls and the Hartmann number M satisfy the relation $c \gg M^{-1/2}$. On the basis of slug and fully developed flow models they predicted that pressure drop in the orifice can become very large because of leakage current effects. Pressure drop in a multiple duct system rapidly increases with the number of channels; it is determined by the ducts close to the center where the flow becomes of Hartmann type (no jets at the side walls)¹. When the number of channels exceeds 20, pressure drop becomes 10 to 100 times higher than that in a single duct, that makes it almost impossible to pump a coolant through the blanket.

The increase of the pressure drop by a factor of 100 is mainly due to the fact that the top wall is thick. A thick wall perpendicular to the magnetic field in the limit $M \rightarrow \infty$ acts like a very good conductor and creates a pressure gradient of the order 1. This is not the case in a duct with thin conducting walls with $c \ll 1$, in which pressure gradient is proportional to c . In the reference concept of blanket the radial ducts have thin conducting walls with wall conductance ratio in the

1

The reader may prefer to use the term "slug flow", or more precise term "flow in a duct with perfectly conducting side walls".

range 0.02+0.04 with FCI and about 10 times these values if FCI are not used. Therefore, pressure drop due to MCE is expected to be much smaller than in a duct with a thick top wall. Nevertheless, MCE is one of the critical issues for the reference concept; it requires thorough consideration.

If $c \gg M^{-1/2}$ all current leaving the core enters side walls; currents carried by the side layers are neglected. In this case the analysis of the flow, especially in three dimensions, simplifies considerably (see [4,5], for example). Even if this relation for blanket-relevant range of parameters does not hold (Hartmann number varies within the range 3000+4000), the assumption $c \gg M^{-1/2}$ is usually made [4,5], which is the basis for the so-called Core-Flow Approximation (CFA). The range of validity of CFA with reference to multiple duct flow is discussed in Sec. 4.

If pressure drops in all channels are equal, MCE results in nonuniform flow distribution among them. One of the possible ways to even that has been suggested by Hua & Picologlou [6], who studied liquid-metal flow through a manifold that fed the array of nine electrically coupled rectangular ducts. On the basis of CFA they found that nonuniform flow partition may be reduced or even eliminated by properly chosen combination of wall conductance ratios.

McCarthy et. al. [4,7] investigate fully-developed flow in multiple thin-walled rectangular ducts in a different context, when applied magnetic field is parallel to the top and bottom and

perpendicular to the side walls and the dividing walls.

In all cited papers, except in the work by Madarame, Taghavi & Tillack [2], variation of pressure drop with channel number has not been studied. Since the number of coolant channels in the reference concept is 29 in inboard and 38 in outboard blankets [3], this dependence becomes very important. Forthcoming experimental studies of MCE in radial-toroidal bends [3] with both electrically coupled and separated radial ducts require theoretical predictions of pressure drops and flow rate distribution among channels for a wide range of flow parameters, namely the Hartmann number, wall conductance ratio, number of channels and duct geometry. The aim of the present paper is to provide such an investigation in the radial branch of a multi-channel bend away from the junction between radial and toroidal ducts, i.e. in the region of fully developed flow. Fully developed multiple channel flow problem is analysed by means of singular perturbation theory as the Hartmann number M tends to infinity. This theory has been successfully applied by many authors to the flow in a single channel [8,9].

Walker [9] treats the flow in a thin-walled duct with all walls having the same wall conductance ratio c with the restriction $M^{-1} \ll c \ll 1$. The solution is obtained for three different cases:

- i) $c \ll M^{-1/2}$,
- ii) $c = O(M^{-1/2})$,
- iii) $c \gg M^{-1/2}$.

In the present paper it is assumed that top and bottom walls have the same wall conductance ratios. The restriction $c \ll 1$, as well as dividing the solution procedure on the three cases i) to iii) are not necessary, and therefore in the present study these restrictions are relaxed. Since top and side wall conductance ratios c_t and c_s have different influence on the flow structure (the increase of c_t results generally in increasing volume flux carried by the side layers, while the effect of increasing c_s is opposite) they are treated as independent parameters. The value of c_s is considered as arbitrary (including limiting cases of insulating and perfectly conducting walls). For the value of c_t the assumption $c_t \gg M^{-1}$, which holds for liquid-metal blankets, is retained in order to keep the side-layer problem tractable by analytical methods. To summarize, the present solution is obtained under the following assumptions:

- i) the applied magnetic field is strong, i.e. $M \gg 1$;
- ii) top and bottom walls have the same wall conductance ratios $c_t = c_b$;
- iii) top and bottom walls are much better conductors than the Hartmann layers, i.e. $c_t \gg M^{-1}$.

2. FORMULATION OF THE PROBLEM

Consider steady flow of a viscous conducting incompressible fluid along n electrically coupled straight rectangular channels of infinite length (see Fig. 1) due to pressure drop imposed in the z -direction. Pressure drop may vary from one channel to the other. A strong uniform external magnetic field $\underline{B}^e = B_o \underline{e}_y$ is applied parallel to channel side walls and perpendicular to the top and the bottom walls. All channels have the same height $2a$. The walls parallel to the magnetic field, i.e. the outside side-walls and the dividing walls, are numbered from 1 to $n+1$ from the left to the right. They have thicknesses $h_s^{(i)}$ and conductivities $\sigma_s^{(i)}$ and are placed at $x=x^{(i)}$ ($i=1, \dots, n+1$). The value of $x^{(1)}$ is set to zero. The distance between the side walls is denoted by $d^{(i)}$, i.e. $d^{(i)} = x^{(i+1)} - x^{(i)}$. The top walls having thicknesses $h_t^{(i)}$ and conductivities $\sigma_t^{(i)}$ are placed at $y=a$ ($i=1, \dots, n$). The problem is symmetric with respect to $y=0$, and hence the flow in the upper half of the duct $y \geq 0$ is considered subject to appropriate symmetry conditions at $y=0$.

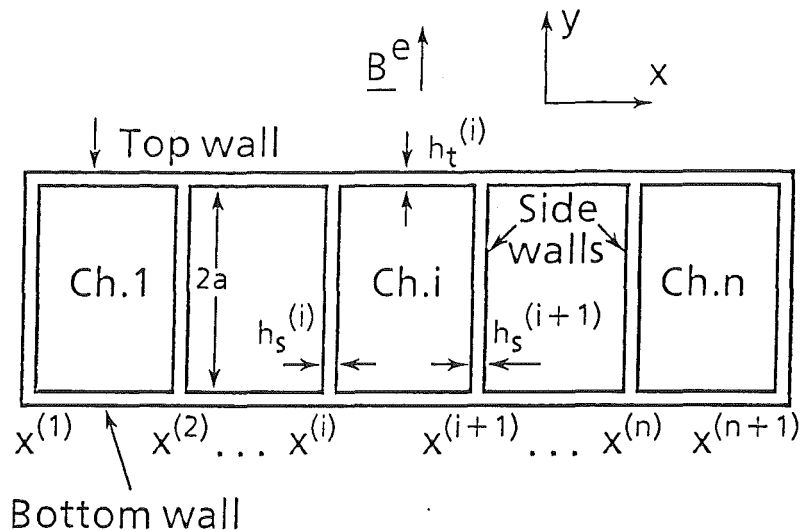


Fig.1 Schematic diagram of the flow in multiple rectangular ducts

2.1 GOVERNING EQUATIONS

The problem can be formulated in terms of fluid velocity and either electric potential or induced magnetic field. In this paper we follow the latter classical formulation for fully developed flow [10]. In this case the dimensionless equations governing the flow in channel i ($i=1, \dots, n$) read

$$\nabla^2 v^{(i)} + M \frac{\partial b^{(i)}}{\partial y} = -k^{(i)} M^2, \quad (2.1a)$$

$$\nabla^2 b^{(i)} + M \frac{\partial v^{(i)}}{\partial y} = 0, \quad (2.1b)$$

where

(x, y, z) is the cartesian coordinate system,

$v^{(i)}, b^{(i)}$ are the fluid velocity and the induced magnetic field, respectively; these are both in the z -direction,

$k^{(i)} = dp_m^{(i)}/dz$ is the pressure gradient,

$p_m^{(i)}$ is the total pressure,

$M = B_0 a (\sigma / \rho \nu)^{1/2}$ is the Hartmann number,

ν, σ, ρ are the kinematic viscosity, density and conductivity of the fluid, respectively,

μ is the magnetic permeability,

$\nabla^2 = \partial^2 / \partial x^2 + \partial^2 / \partial y^2$ is the Laplace operator.

The length, the fluid velocity, the induced magnetic field and the pressure are normalized by a, v_0 (characteristic fluid velocity,

which will be determined later), $\mu v_o (\rho\nu\sigma)^{1/2}$, $\sigma a v_o B_o^2$, respectively.

Once the functions $v^{(i)}$ and $b^{(i)}$ are known, the electric current density $\underline{j}^{(i)}$ (normalized by $v_o B_o \sigma$) and the electric potential $\Phi^{(i)}$ (normalized by $v_o B_o a$) can be calculated from Ampère's law

$$\begin{aligned} \underline{j}^{(i)} &= M^{-1} \text{curl} \left[b^{(i)} \underline{e}_z \right] = \\ &= M^{-1} \frac{\partial b^{(i)}}{\partial y} \underline{e}_x - M^{-1} \frac{\partial b^{(i)}}{\partial x} \underline{e}_y, \end{aligned} \quad (2.2a)$$

and Ohm's law

$$\begin{aligned} \nabla \Phi^{(i)} &= - \underline{j}^{(i)} + (v^{(i)} \underline{e}_z) \times \underline{B}^e = \\ &= \left[-M^{-1} \frac{\partial b^{(i)}}{\partial y} - v^{(i)} \right] \underline{e}_x + M^{-1} \frac{\partial b^{(i)}}{\partial x} \underline{e}_y. \end{aligned} \quad (2.2b)$$

From equation (2.2a) it follows that the function $b^{(i)}$ is a stream function for the vector field $\underline{j}^{(i)}$. Hence, lines of constant $b^{(i)}$ are electric current lines.

2.1 BOUNDARY CONDITIONS

The boundary conditions for the fluid velocity are the non-slip conditions on the walls. If duct walls are thin, i.e. the wall thickness h_w satisfies the relation $h_w \ll 1$, the thin-wall condition

$$c_w \frac{\partial b}{\partial \underline{n}} = b \quad (2.3a)$$

holds on the fluid-wall interface [11], where \underline{n} is unit vector normal to the wall, into the fluid; $c_w = \sigma_w h_w / \sigma a$ is the wall conductance ratio. The thin-wall condition is not valid at duct corners, where the two thin walls carrying currents in directions perpendicular one to the other join. However, the effect of the corners is local and in most cases has no influence on the flow in the bulk of the fluid [12]. The thin-wall condition (2.3a) was obtained by assuming that a solid wall separates conducting fluid from insulating medium. If a wall separates two regions occupied by conducting fluids with the same properties (see Fig. 2), the similar reasoning as that used by Shercliff [11] leads to the two conditions

$$c_w \frac{\partial b^{(1)}}{\partial \underline{n}_1} = b^{(1)} - b^{(2)}, \quad (2.3b)$$

$$\frac{\partial b^{(1)}}{\partial \underline{n}_1} = - \frac{\partial b^{(2)}}{\partial \underline{n}_2}, \quad (2.3c)$$

where unit vector \underline{n}_j is normal to the wall, into the region j ; $b^{(j)}$ is the induced magnetic field in the region j ($j=1,2$). The equation (2.3c),

together with (2.2a), indicates that tangential component of the electric current in the fluid is continuous across the wall. The equation (2.3b) determines the value of this current, which is proportional to the jump of the induced magnetic field across the wall. If a wall is a perfect conductor, i.e. $c_w \Rightarrow \infty$, the conditions (2.3b) and (2.3c) lead to $\partial b^{(1)}/\partial \underline{n}_1 = \partial b^{(2)}/\partial \underline{n}_2 = 0$, which hold also in Shercliff's case. However, if $c_w \Rightarrow 0$, the condition (2.3b) becomes $b^{(1)} = b^{(2)}$, i.e. the induced magnetic field, together with the normal component of the electric current, become continuous across the wall. In contrast to the Shercliff's case in the limit $c_w \Rightarrow 0$ the wall does not become insulating because it separates two conducting media, and hence electric current can cross the wall with no resistance. In this limit the wall should be considered of zero thickness still being electrically conducting.

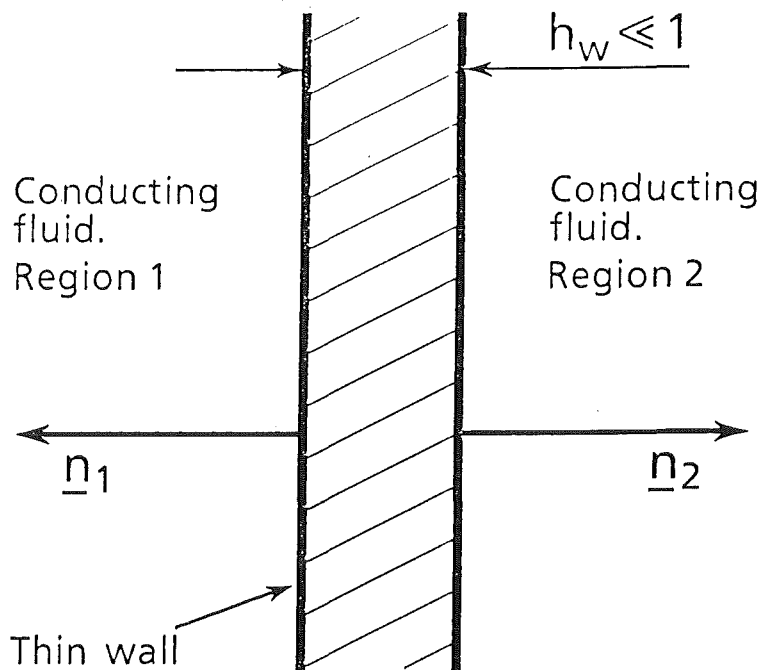


Fig. 2 Thin wall dividing two regions of conducting fluid

For the present geometry condition (2.3a) holds on the outside side walls and the top wall, whereas the conditions (2.3b) and (2.3c) hold on the dividing walls.

When applied to the channel i ($i=1, \dots, n$), the non-slip conditions, the conditions (2.3) and the symmetry conditions with respect to y give

$$v^{(i)}=0, \quad c_s^{(i)} \frac{\partial b^{(i)}}{\partial x} = b^{(i)} - \delta_i b^{(i-1)} \quad \text{at } x=x^{(i)}, \quad (2.1c,d)$$

$$\partial b^{(i)} / \partial x = \partial b^{(i-1)} / \partial x \quad \text{at } x=x^{(i)}, \quad i \neq 1, \quad (2.1e)$$

$$v^{(i)}=0, \quad c_s^{(i+1)} \frac{\partial b^{(i)}}{\partial x} = -b^{(i)} + \epsilon_i b^{(i+1)} \quad \text{at } x=x^{(i+1)}, \quad (2.1f,g)$$

$$\partial b^{(i)} / \partial x = \partial b^{(i+1)} / \partial x \quad \text{at } x=x^{(i+1)}, \quad (2.1h)$$

$$v^{(i)}=0, \quad c_t^{(i)} \frac{\partial b^{(i)}}{\partial y} = -b^{(i)} \quad \text{at } y=1, \quad (2.1i,j)$$

$$\frac{\partial v^{(i)}}{\partial y} = 0, \quad b^{(i)}=0 \quad \text{at } y=0, \quad (2.1k,l)$$

where

$$\delta_i = \begin{cases} 0 & \text{for } i = 1 \\ 1 & \text{for } i \neq 1 \end{cases}, \quad \epsilon_i = \begin{cases} 1 & \text{for } i \neq n \\ 0 & \text{for } i = n \end{cases},$$

$$\text{and } c_t^{(i)} = \frac{\sigma_t^{(i)} h_t^{(i)}}{\sigma a}, \quad c_s^{(i)} = \frac{\sigma_s^{(i)} h_s^{(i)}}{\sigma a}, \quad c_s^{(i+1)} = \frac{\sigma_s^{(i+1)} h_s^{(i+1)}}{\sigma a}$$

are the top-, the left-, and the right- wall conductance ratios of channel i , respectively.

In duct flows either pressure gradients $k^{(i)}$ or flow rates $Q^{(i)}$ in each channel are specified. If pressure gradients are fixed, the flow rates are calculated from the equations

$$Q^{(i)} = 2 \int_0^1 dy \int_{x^{(i)}}^{x^{(i+1)}} v^{(i)} dx. \quad (2.4)$$

For given flow rates $Q^{(i)}$ the expression (2.4) provides the system of equations for the determination of pressure gradients. In both cases the characteristic velocity v_0 is defined as average velocity in the whole duct, i.e.

$$\sum_{i=1}^n Q^{(i)} = 2x^{(n+1)}. \quad (2.5)$$

3. ASYMPTOTIC SOLUTION

The problem (2.1) is treated by means of matched asymptotics. According to this method the flow region is divided into the following subregions (Fig. 3):

- (C_i) the inviscid core regions,
- (H_i) the Hartmann boundary layers near the top wall adjacent to the cores with $O(M^{-1})$ thickness,
- (SR_i) , (SL_i) the side layers at the side walls; these are of $O(M^{-1/2})$ thickness,
- (HS) the Hartmann layers near the top wall adjacent to the side layers, with a thickness of $O(M^{-1})$ and a length of $O(M^{-1/2})$.

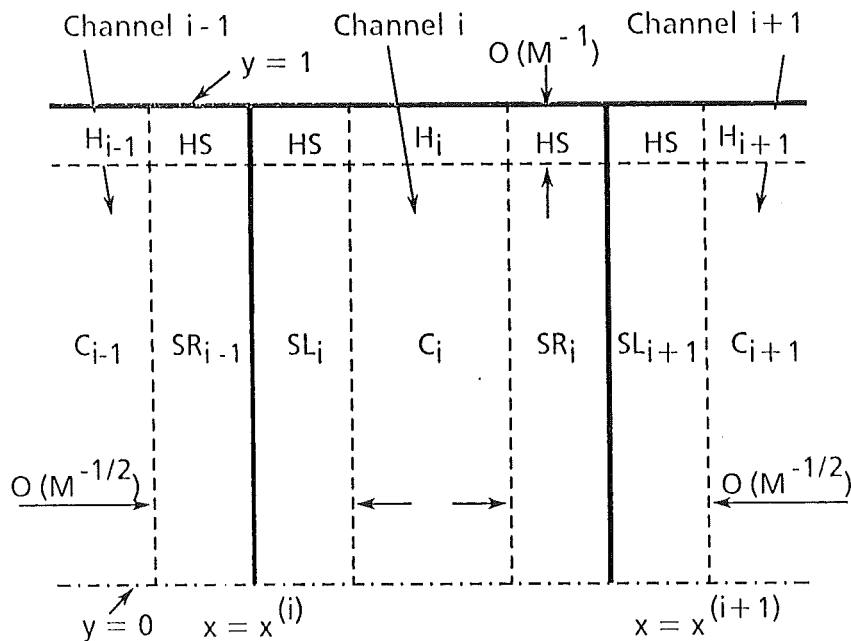


Fig. 3 Flow subregions at large Hartmann number

In addition, there are regions with both dimensions of $O(M^{-1})$ at the channel corners. They need not to be analysed in detail for the determination of the leading term in each asymptotic expansion for the other regions [13].

3.1 THE CORE C AND THE HARTMANN LAYER H

In regions C_i and H_i the flow is essentially one-dimensional. The velocity and the induced magnetic field do not depend on the variable x , and the flow is the same as the Hartmann flow. The flow in the core and adjacent Hartmann layer is described by the functions [8]

$$v_c^{(i)} = k^{(i)} \eta_i, \quad (3.1a)$$

$$b_c^{(i)} = -k^{(i)} My, \quad (3.1b)$$

$$v_H^{(i)} = v_c^{(i)} (1 - e^{-y_H}), \quad (3.2a)$$

$$b_H^{(i)} = b_c^{(i)} + v_c^{(i)} e^{-y_H}, \quad (3.2b)$$

where $y_H = M(y-1)$ is the stretched Hartmann-layer variable and

$$\eta_i = \frac{1 + c_t^{(i)}}{c_t^{(i)} + M^{-1}}.$$

While deriving formulas (3.2) the only assumption has been made that $M \gg 1$, and exponentially small terms only have been neglected. The

functions $v_H^{(i)}$ and $b_H^{(i)}$ are composite asymptotic expansions, which are valid in regions C_i and H_i to any order in M .

The functions (3.1) determine the flow in the cores of all channels. However, these functions evidently fail to describe the flow near the side walls parallel to the magnetic field lines where side layers appear, which carry part of the volume flux.

3.2 SIDE LAYERS SR AND SL

In each channel of the multiple duct there are two side layers. One of them is at the left wall with number i (region SL_i); the other one is at the right wall with number $i+1$ (region SR_i). The thickness of both layers is of the order of $M^{-1/2}$. If the channel width $d^{(i)}$ is of the same order, the core disappears and the two side layers merge into a single one. This case is not covered by the present investigation, and special but straightforward treatment is necessary. However, in the reference concept of liquid-metal blanket radial ducts have square cross-section, so that in the present paper $d^{(i)}$ is supposed to be of the order 1. Under this condition the two layers split, and may be treated separately.

Consider side-layers at the wall i , which is the left side wall of channel i and the right side wall of channel $i-1$. In contrast to the core, the flow in the side layer near the wall i must be treated in channels i and $i-1$ simultaneously due to coupling between the induced

magnetic fields in these channels (see 2.3d,e,g,h).

The vicinity of the side wall $x=x^{(i)}$ is stretched by introducing a variable

$$\xi_i = M^{1/2} \left[x - x^{(i)} \right]. \quad (3.3)$$

Substituting (3.3) into equations (2.1a,b) and similar equations governing the flow in channel $i-1$ and keeping main terms in these equations as $M \Rightarrow \infty$ gives

$$\frac{\partial^2 v_{SL}^{(i)}}{\partial \xi_i^2} + \frac{\partial b_{SL}^{(i)}}{\partial y} = -k^{(i)} M, \quad (3.4a)$$

$$\frac{\partial^2 b_{SL}^{(i)}}{\partial \xi_i^2} + \frac{\partial v_{SL}^{(i)}}{\partial y} = 0, \quad \text{for } \xi_i \geq 0; \quad (3.4b)$$

and

$$\frac{\partial^2 v_{SR}^{(i-1)}}{\partial \xi_i^2} + \frac{\partial b_{SR}^{(i-1)}}{\partial y} = -k^{(i-1)} M, \quad (3.4c)$$

$$\frac{\partial^2 b_{SR}^{(i-1)}}{\partial \xi_i^2} + \frac{\partial v_{SR}^{(i-1)}}{\partial y} = 0, \quad \text{for } \xi_i \leq 0. \quad (3.4d)$$

The boundary conditions for the system (3.4a-d) with respect to ξ_i are obtained from the conditions (2.1c-e) on the wall i and the conditions of matching the core-flow solutions in channels i and $i-1$.

These give

$$v_{SL}^{(i)} = 0, \quad v_{SR}^{(i-1)} = 0 \quad \text{at } \xi_i = 0, \quad (3.4e, f)$$

$$c_s^{(i)} M^{1/2} \frac{\partial b_{SL}^{(i)}}{\partial \xi_i} = b_{SL}^{(i)} - \delta_i b_{SR}^{(i-1)}, \quad \text{at } \xi_i = 0; i \neq n+1, \quad (3.4g)$$

$$c_s^{(i)} M^{1/2} \frac{\partial b_{SR}^{(i-1)}}{\partial \xi_i} = \epsilon_i b_{SL}^{(i)} - b_{SR}^{(i-1)}, \quad \text{at } \xi_i = 0; i \neq 1, \quad (3.4h)$$

$$v_{SL}^{(i)} \Rightarrow v_c^{(i)}, \quad b_{SL}^{(i)} \Rightarrow b_c^{(i)} \quad \text{as } \xi_i \Rightarrow \infty, \quad (3.4i, j)$$

$$v_{SR}^{(i-1)} \Rightarrow v_c^{(i-1)}, \quad b_{SR}^{(i-1)} \Rightarrow b_c^{(i-1)} \quad \text{as } \xi_i \Rightarrow -\infty. \quad (3.4k, l)$$

The conditions for the system (3.4a-d) with respect to y are the symmetry conditions

$$\frac{\partial v_{SL}^{(i)}}{\partial y} = 0, \quad b_{SL}^{(i)} = 0 \quad \text{at } y=0, \xi_i \geq 0, \quad (3.4m, n)$$

$$\frac{\partial v_{SR}^{(i-1)}}{\partial y} = 0, \quad b_{SR}^{(i-1)} = 0 \quad \text{at } y=0, \xi_i \leq 0, \quad (3.4o, p)$$

and the boundary conditions at $y=1$ which are obtained from the conditions of matching with the Hartmann layer (region HS) variables (see Appendix A). They read

$$v_{SL}^{(i)} \left[1 + M c_t^{(i)} \right] + b_{SL}^{(i)} = k^{(i)} M \left[1 + c_t^{(i)} \right] \quad \text{at } y=1, \xi_i \geq 0, \quad (3.4q)$$

$$v_{SR}^{(i-1)} \left[1 + M c_t^{(i-1)} \right] + b_{SR}^{(i-1)} = k^{(i-1)} M \left[1 + c_t^{(i-1)} \right] \quad \text{at } y=1, \xi_i \leq 0. \quad (3.4r)$$

The equations (3.4) constitute the problem governing the flow in the shear layers at the wall i . By this moment no assumption has been made on the values of wall conductance ratios. An analytic solution to the problem (3.4) can be obtained if $Mc_t^{(i)} \gg 1$ for all i , i.e. the top (and the bottom) walls of all channels are much better conductors than the Hartmann layers. Under this assumption conditions (3.4q) and (3.4r) become

$$v_{SL}^{(i)} = v_c^{(i)} \quad \text{at } y=1, \xi_i \geq 0, \quad (3.4q')$$

$$v_{SR}^{(i-1)} = v_c^{(i-1)} \quad \text{at } y=1, \xi_i \leq 0. \quad (3.4r')$$

The solution to the problem (3.4) obtained by means of finite Fourier transform with respect to y reads

$$v_{SL}^{(i)} = v_c^{(i)} + \sum_{j=0}^{\infty} V_L^{(i,j)}(\xi_i) \cos \beta_j y, \quad (3.5a)$$

$$b_{SL}^{(i)} = b_c^{(i)} + \sum_{j=0}^{\infty} B_L^{(i,j)}(\xi_i) \sin \beta_j y, \quad (3.5b)$$

$$v_{SR}^{(i-1)} = v_c^{(i-1)} + \sum_{j=0}^{\infty} V_R^{(i-1,j)}(\xi_i) \cos \beta_j y, \quad (3.5c)$$

$$b_{SR}^{(i-1)} = b_c^{(i-1)} + \sum_{j=0}^{\infty} B_R^{(i-1,j)}(\xi_i) \sin \beta_j y, \quad (3.5d)$$

where

$$V_{L,R}^{(i,j)}(\xi_i) = \exp(-\gamma_j |\xi_i|) \left[C_{L,R}^{(i,j)} \sin \gamma_j |\xi_i| + D^{(i,j)} \cos \gamma_j |\xi_i| \right],$$

$$B_{L,R}^{(i,j)}(\xi_i) = \exp(-\gamma_j |\xi_i|) \left[C_{L,R}^{(i,j)} \cos \gamma_j |\xi_i| - D^{(i,j)} \sin \gamma_j |\xi_i| \right],$$

$$C_L^{(i,j)} = \frac{\omega_j \sqrt{M}}{\beta_j \left[\delta_{i+1} + \alpha_{ij} \sqrt{M} \right]} \left\{ \sqrt{M} \left[k^{(i)} - \delta_i k^{(i-1)} \right] - v_c^{(i)} \beta_j \alpha_{ij} \right\},$$

$$C_R^{(i,j)} = \frac{\omega_j \sqrt{M}}{\beta_j \left[\epsilon_{i+1} + \alpha_{i+1,j} \sqrt{M} \right]} \left\{ \sqrt{M} \left[k^{(i)} - \epsilon_i k^{(i+1)} \right] - v_c^{(i)} \beta_j \alpha_{i+1,j} \right\},$$

$$D^{(i,j)} = v_c^{(i)} \omega_j, \quad \beta_j = \left[j + \frac{1}{2} \right] \pi, \quad \gamma_j = \sqrt{\beta_j / 2},$$

$$\omega_j = 2(-1)^j \beta_j^{-1}, \quad \alpha_{ij} = c_s^{(i)} \gamma_j.$$

While deriving the solution (3.5) terms $O(M^{-1/2})$ have been neglected with respect to those retained. Throughout this paper this is done all the time when it is possible.

The second terms in the right hand side of each of the equations (3.5a) to (3.5d) represent the excess of the side-layer velocity and the induced magnetic field over the core ones. If $c_s^{(i)} = \infty$, these terms are of the order 1; if $c_s^{(i)} = 0$, they are of the order \sqrt{M} . It holds for layers

at both outside and dividing walls provided the difference between pressure gradients in the neighbouring channels is of the order 1.

3.3 COMPOSITE SOLUTION AND FLOW RATES

If pressure gradients $k^{(i)}$ are specified, the equations (3.1), (3.2), (3.5) and the solution to the problem governing the flow in the layer HS (see Appendix A) give

$$v^{(i)} = \left[v_{SL}^{(i)} + v_{SR}^{(i)} - v_C^{(i)} \right] \left[1 - \exp(y_H) \right], \quad (3.6a)$$

$$b^{(i)} = \left[b_{SL}^{(i)} + b_{SR}^{(i)} - b_C^{(i)} \right] \left[1 - \exp(y_H) \right]. \quad (3.6b)$$

These expressions represent the unique first-order asymptotic solution to the problem (2.1) in the whole duct apart from the corners.

The volume flux carried by the core, the left and the right side layers, calculated by integrating equation (3.1a) over the cross-section of channel i , and the equations (3.5a) and (3.5c) over the side layer regions, are

$$Q_C^{(i)} = 2k^{(i)} \eta_i d_i, \quad (3.7a)$$

$$Q_{SL}^{(i)} = M^{-1/2} Q_C^{(i)} +$$

$$+ \sqrt{2M} \left[k^{(i)} - \delta_i k^{(i-1)} \right] \sum_{j=0}^{\infty} \beta_j^{-7/2} (1 + \delta_i + \alpha_{i,j} \sqrt{M})^{-1}, \quad (3.7b)$$

$$Q_{SR}^{(i)} = M^{-1/2} Q_C^{(i)} +$$

$$+ \sqrt{2M} \left[k^{(i)} - \epsilon_i k^{(i+1)} \right] \sum_{j=0}^{\infty} \beta_j^{-7/2} (1 + \epsilon_i + \alpha_{i+1,j} \sqrt{M})^{-1}. \quad (3.7c)$$

Total flow rate in the channel i is equal to the sum of the three flow rates, i.e.

$$Q^{(i)} = Q_C^{(i)} + Q_{SL}^{(i)} + Q_{SR}^{(i)}. \quad (3.8)$$

If the difference between pressure gradients in neighbouring channels is of the order $M^{-1/2}$, or the side-wall is perfectly conducting, both side-layer volume fluxes $Q_{SL}^{(i)}$ and $Q_{SR}^{(i-1)}$ at this wall are negligible compared to core one. In the other cases the first terms in the right-hand side of the equations (3.7b) and (3.7c) are negligible with respect to the second ones. Side-layer volume fluxes at the wall i become proportional to the difference between pressure gradients and are of opposite sign, since $Q_{SL}^{(i)} = -Q_{SR}^{(i-1)}$. If left side layer in channel i carries volume flux in the main-flow direction, the flow in the right side-layer in channel $i-1$ is reversed, and vice versa.

The side-layer volume fluxes $Q_{SL}^{(i)}$ and $Q_{SR}^{(i)}$ may be expressed in terms of side-wall currents by integrating equations (3.4b) and (3.4d)

with respect to ξ_i once and with respect to y twice, taking into account the boundary conditions (3.4q') and (3.4r'). This gives

$$Q_{\text{SL}}^{(i)} = M^{-1/2} Q_{\text{C}}^{(i)} + \int_0^1 dy \int_y^1 j_{\text{y,SL}}(x^{(i)}, t) dt, \quad (3.9a)$$

$$Q_{\text{SR}}^{(i)} = M^{-1/2} Q_{\text{C}}^{(i)} + \int_0^1 dy \int_y^1 j_{\text{y,SR}}(x^{(i)}, t) dt, \quad (3.9b)$$

where

$$j_{\text{y,SL}}(x^{(i)}, y) = \sqrt{2} \left[k^{(i)} - \delta_i k^{(i-1)} \right] \sum_{j=0}^{\infty} \frac{(-1)^j \sin \beta_j y}{\beta_j^{3/2} \left[\delta_{i+1} + \alpha_{i,j} \sqrt{M} \right]}, \quad (3.9c)$$

and

$$j_{\text{y,SR}}(x^{(i)}, y) = \sqrt{2} \left[k^{(i)} - \epsilon_i k^{(i+1)} \right] \sum_{j=0}^{\infty} \frac{(-1)^j \sin \beta_j y}{\beta_j^{3/2} \left[\epsilon_{i+1} + \alpha_{i+1,j} \sqrt{M} \right]} \quad (3.9d)$$

are tangential to the wall components of the electric current estimated on the right and the left wall surfaces, respectively. From (3.9a) and (3.9b) it follows that the flow rate carried by a side layer is proportional to the average amount of the electric current carried by the wall in the y -direction.

If pressure gradients are unknown, but the flow rates are given, substituting the expression (3.8) into the equation (2.4) results in a three-diagonal system of linear algebraic equations for the determination of pressure gradients, namely

$$\delta_i A_{i-1,i} k^{(i-1)} + A_{i,i} k^{(i)} + \epsilon_i A_{i+1,i} k^{(i+1)} = Q^{(i)}, \quad (3.10)$$

where

$$A_{i-1,i} = -2^{3/2} \sqrt{M} \sum_{j=0}^{\infty} \beta_j^{-7/2} (1 + \delta_i + \alpha_{i,j} \sqrt{M})^{-1},$$

$$A_{i+1,i} = -2^{3/2} \sqrt{M} \sum_{j=0}^{\infty} \beta_j^{-7/2} (1 + \epsilon_i + \alpha_{i+1,j} \sqrt{M})^{-1},$$

$$A_{i,i} = 2d_i \eta_i - A_{i-1,i} - A_{i+1,i}.$$

4. RESULTS AND DISCUSSION

For the sake of simplicity in the following discussion we assume that the flow is symmetric with respect to duct's midplane $x=x^{(n+1)}/2$.

4.1 SINGLE CHANNEL

In a single symmetric duct ($n=1$, $c_s^{(1)}=c_s^{(2)}=c_s$, $d^{(1)}=d$, $Q^{(1)}=2d$, $c_t^{(1)}=c_t$) the volume flux carried by each side layer is

$$Q_{SL}^{(1)}=Q_{SR}^{(1)}=k^{(1)}\sqrt{2}\sqrt{M}\sum_{j=0}^{\infty}\beta_j^{-7/2}(1+c_s\gamma_j\sqrt{M})^{-1}. \quad (4.1a)$$

Typical M-shape velocity profile with distinct core and side layers at both side walls is shown on Fig. 4.

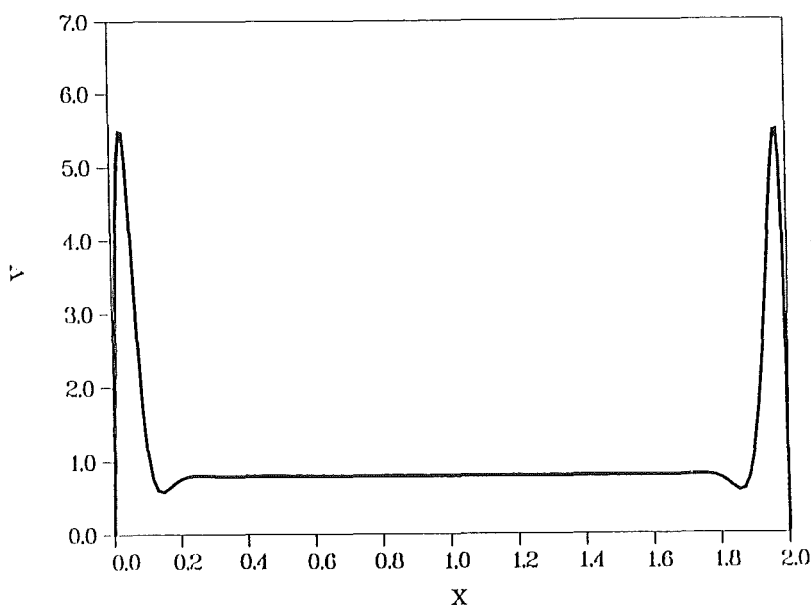


Fig. 4. Fluid velocity in a single duct ($n=1$) at $y=0$. Here $c_t^{(1)}=c_s^{(1)}=c_s^{(2)}=0.1$; $d^{(i)}=2$; $M=1000$.

The equation (3.10) gives

$$k^{(1)} = d \left\{ d \frac{1+c_t}{c_t} + 2^{3/2} \sqrt{M} \sum_{j=0}^{\infty} \beta_j^{-7/2} (1+c_s \gamma_j \sqrt{M})^{-1} \right\}^{-1}. \quad (4.1b)$$

For $c=c_t=c_s$, provided $c \ll 1$, the expression (4.1b) reduces to Walker's one for the pressure gradient in his case ii), i.e. for $c=O(M^{-1/2})$.

If $c_s \gg M^{-1/2}$ (core-flow approximation), the equation (4.1b) leads to a well-known formula for the pressure gradient

$$k^{(1)} = \left\{ 1 + \frac{1}{c_t} + \frac{2}{3dc_s} \right\}^{-1} \quad (4.2a)$$

(see [14], for example). The volume fluxes carried by the side layers in this case are

$$Q_{SL}^{(1)} = Q_{SR}^{(1)} = \left\{ 3c_s \left[1 + \frac{1}{c_t} \right] + \frac{2}{d} \right\}^{-1}. \quad (4.2b)$$

From (4.2a) it follows that as $c_s \Rightarrow 0$ the value of $k^{(1)}$ also tends to zero, which means that in this limit the approximation $c_s \gg M^{-1/2}$ is not valid. Instead, the expression (4.1) for $c_s=0$ gives the value

$$k^{(1)} = \frac{dc_t}{d + 2\zeta c_t \sqrt{M}}, \quad (4.3)$$

where $\zeta = 0.299$. If in addition $c_t \sqrt{M} \gg 1$, i.e. the Hartmann wall and the core are much better conductors than the side layers, the resistance for the electric current is mainly determined by the latter. Then formula (4.3) reduces to that by Hunt [15]

$$k^{(1)} = \frac{d}{2\zeta} M^{-1/2}, \quad (4.4)$$

i.e. the pressure gradient becomes independent of c_t and the top and bottom walls may be treated as perfect conductors. The magnitude of the core velocity is of $O(M^{-1/2})$ and the side layers carry all volume flux.

4.2 TWO CHANNELS

If a duct is divided into two channels ($n=2$, $c_s^{(1)}=c_s^{(2)}=c_s$, $d_1=d_2=d$, $Q^{(1)}=Q^{(2)}=2d$, $c_t^{(1)}=c_t^{(2)}=c_t$), the symmetry conditions $\partial b^{(1)}/\partial x = \partial b^{(2)}/\partial x = 0$ hold at the dividing wall $x=x^{(2)}$. These conditions are the same as those for a perfectly conducting wall. The wall conductance ratio $c_s^{(2)}$ does not enter the problem, and therefore, the dividing wall acts like a perfect conductor. As a result there are no jets at the middle side wall, the side layers at this wall carry no $O(1)$ volume flux, and the only role of the side layers is to satisfy the non-slip condition at the dividing wall (see Fig. 5). The two-channel duct behaves like a single duct of the width $2d$, and the pressure gradients in both channels in the case $c_s \gg M^{-1/2}$ are obtained from (4.2a) to give

$$k^{(1)}=k^{(2)} = \left\{ 1 + \frac{1}{c_t} + \frac{1}{3dc_s} \right\}^{-1}. \quad (4.5)$$

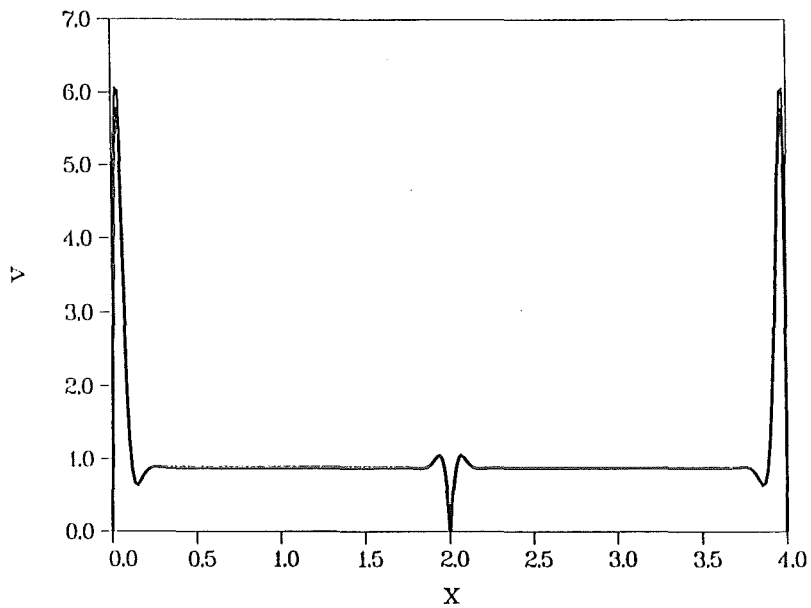


Fig.5. Fluid velocity in a duct divided into two channels ($n=2$) at $y=0$. Here $c_t^{(i)}=c_s^{(i)}=0.1$; $d^{(i)}=2$ for all i ; $M=1000$.

Similar results to those in a previous section for different combinations of wall conductance ratios and the Hartmann number may be obtained for a two-channel duct by substituting $2d$ instead of d .

4.3 THREE CHANNELS AND MORE

Consider first the flow with equal pressure gradients in all channels. In this case the volume fluxes carried by the side layers at the dividing walls are much smaller than those carried by the cores. Therefore, in the middle channel the flow is of Hartmann type (no jets

at the side walls). If top wall conductance ratios are equal, the core velocity is continuous across the dividing walls. The average velocity in the outer channels is higher than in the middle one because two side layers at the outside side walls carry part of a volume flux. The flow structure is qualitatively the same as that in a single channel having width $d = d^{(1)} + d^{(2)} + d^{(3)}$, except that velocity takes zero value at the dividing walls. Therefore, formula (4.1b) applies for calculating pressure gradient.

Consider now the case of fixed flow rates. Without loss of generality we may assume that they are equal and that channels have square cross-section, i. e. $d^{(i)} = 2$ for all i .

If $c_s^{(i)} \gg M^{-1/2}$, an explicit solution of the system (3.10) is easy to obtain in a compact form. It reads

$$k^{(1)} = k^{(3)} = 9c_s^{(1)} \Delta^{-1} \left\{ 2c_s^{(2)} \frac{1+c_t^{(2)}}{c_t^{(2)}} + 1 \right\}, \quad (4.6a)$$

$$k^{(2)} = 3\Delta^{-1} \left\{ 3c_s^{(1)} + c_s^{(2)} \left[6c_s^{(1)} \frac{1+c_t^{(1)}}{c_t^{(1)}} + 1 \right] \right\}, \quad (4.6b)$$

where

$$\Delta = \left\{ 3c_s^{(2)} \frac{1+c_t^{(2)}}{c_t^{(2)}} + 1 \right\} \left\{ 6c_s^{(1)} \frac{1+c_t^{(1)}}{c_t^{(1)}} + 1 \right\} + 3 \frac{1+c_t^{(2)}}{c_t^{(2)}} c_s^{(1)}.$$

Volume fluxes carried by the side layers are

$$Q_{sL}^{(1)} = \frac{1}{3c_s^{(1)}} k^{(1)}, \quad (4.7a)$$

$$Q_{sL}^{(2)} = -Q_{sR}^{(1)} = \frac{1}{3c_s^{(2)}} \left[k^{(2)} - k^{(1)} \right]. \quad (4.7b)$$

On the basis of the expressions (4.6) and (4.7) the most essential features of the MCE in the case of fixed flow rates may be described.

When electrically conducting fluid flows across magnetic field lines, the electric current $\sigma \underline{v}_x \times \underline{B}^e$ is induced by the core velocity of each channel in the $-x$ -direction (see Fig. 6). The electric circuit conducting current consists of cores, side walls, side layers and top and bottom walls of all channels. Electrical conductance of the circuit determines the values of the induced currents, which in turn determine pressure gradients in all channels, since $\underline{j}_c^{(i)} = -\underline{e}_x k^{(i)}$ (eq. 2.2a and 3.1b). Due to the assumptions imposed the Hartmann layers conduct negligibly small currents and thus play no role for the determination of pressure gradient. Side walls and side layers represent parallel resistance to the electric current in the y -direction. If $c_s^{(i)} \gg M^{-1/2}$, i.e. side walls are much better conductors than the side layers, the latter may also be excluded from consideration. All current induced in the core enters the side walls and the conductance of the circuit is determined by wall conductance ratios.

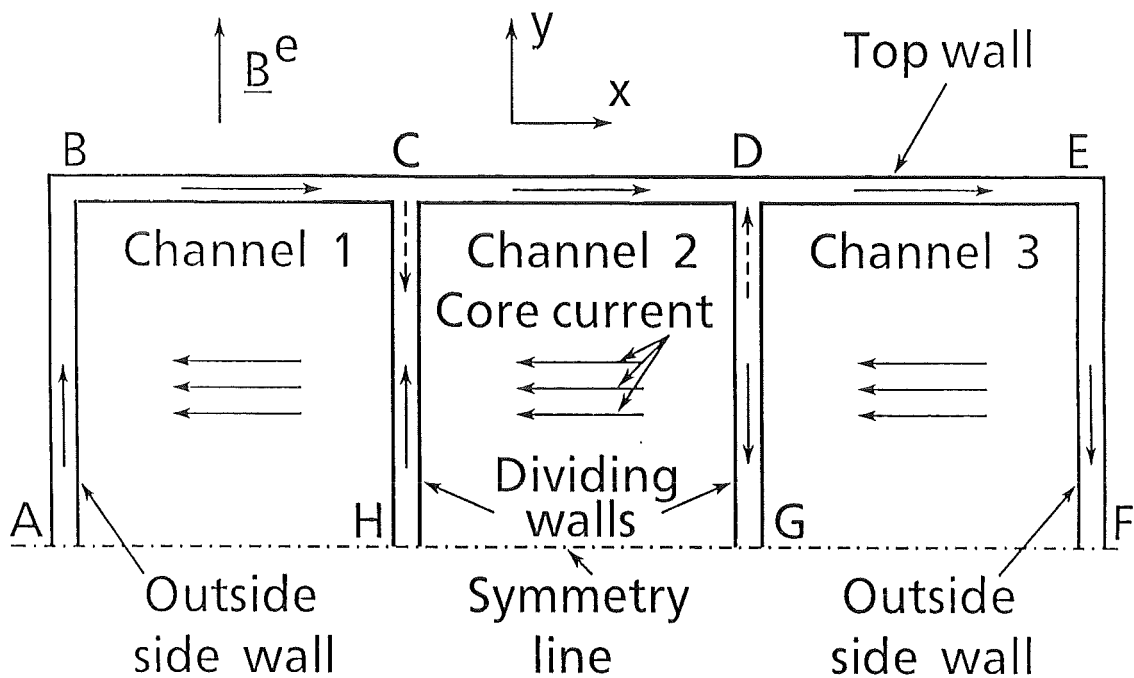


Fig. 6 Schematic diagram of electric currents in a duct divided into three channels.

Since channels are electrically connected, the induced current can cross all of them and complete its circuit in the outside side-walls of the outer channels and the top wall (path ABCDEFGHA). If there were no dividing walls, the electric current would flow as a uniform core current from one outside side wall to the other. In the presence of electrically conducting dividing walls part of the induced current may flow along them in the y (or $-y$) - direction. Consider wall CH dividing channels 1 and 2. If channels 1 and 2 were separated, the electric current induced in channel 1 would flow in the direction \overline{CH} , whereas the current induced in channel 2 - in the direction \overline{HC} . Since the dividing wall CH is thin and the current flowing along it must be uniform, parts of the currents induced in channels 1 and 2 cancel because of their

opposite directions². The remaining current is proportional to the difference between the core currents induced in channels 1 and 2, or equivalently, to the absolute value of the difference between pressure gradients $|k^{(1)} - k^{(2)}|$. The direction of this current and the sign of the side-layer volume flux at the dividing walls are determined by the sign of this difference (see 4.7b). If $k^{(2)} > k^{(1)}$ (current induced in channel 2 is stronger), the wall current is in the direction \overline{HC} and an additional current path is HCDGH. The fluid at the dividing wall flows in the main-flow direction in the channel 2, whereas in the side layer of channel 1 the flow is reversed (see Fig. 7). If $k^{(2)} < k^{(1)}$, the current is in the direction \overline{CH} ; an additional current path is HGDCH and the flow direction at the wall is opposite to the previous case (Fig.8). From (4.6) follows that the sign of the value $k^{(2)} - k^{(1)}$ is determined by the sign of the expression

$$\Gamma = c_s^{(2)} \left\{ 6c_s^{(1)} \left[\frac{1}{c_t^{(1)}} - \frac{1}{c_t^{(2)}} \right] + 1 \right\}. \quad (4.8)$$

The value of Γ may be considered as the measure of the difference between conductances of the two circuits. If $c_t^{(2)} = c_t^{(1)}$, Γ is positive, i.e. $k^{(2)} > k^{(1)}$. Pressure gradients in all channels are equal if $\Gamma=0$.

²In a thick wall electric currents can flow in opposite directions without interaction.

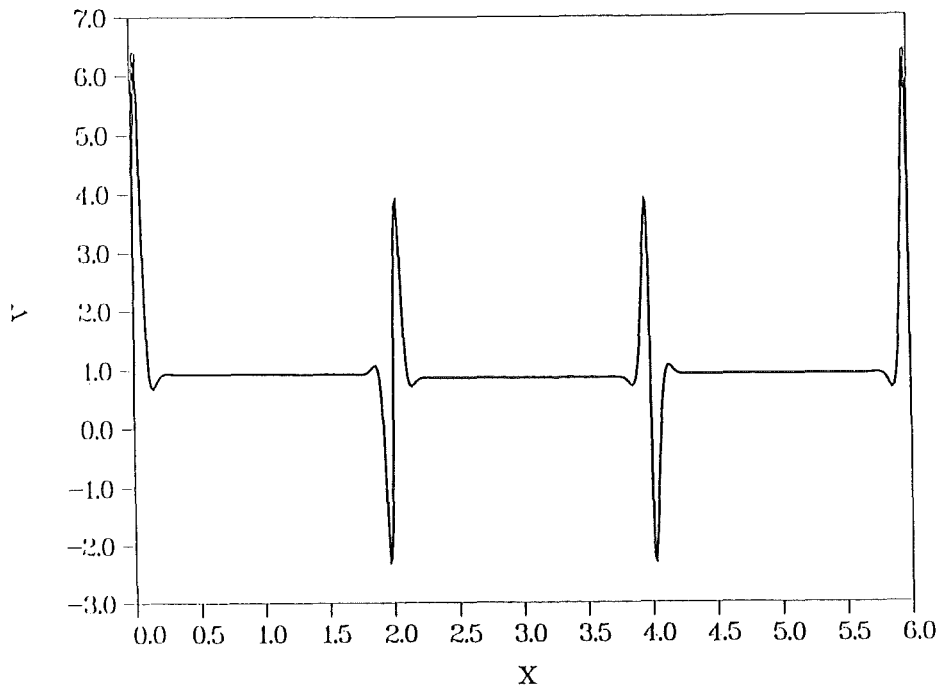


Fig. 7. Fluid velocity in a duct divided into three channels ($n=3$; fixed flow rates) at $y=0$. Here $c_t^{(1)}=c_t^{(3)}=0.1$; $c_t^{(2)}=0.2$; $c_s^{(i)}=0.1$; $d^{(i)}=2$ for all i ; $M=1000$.

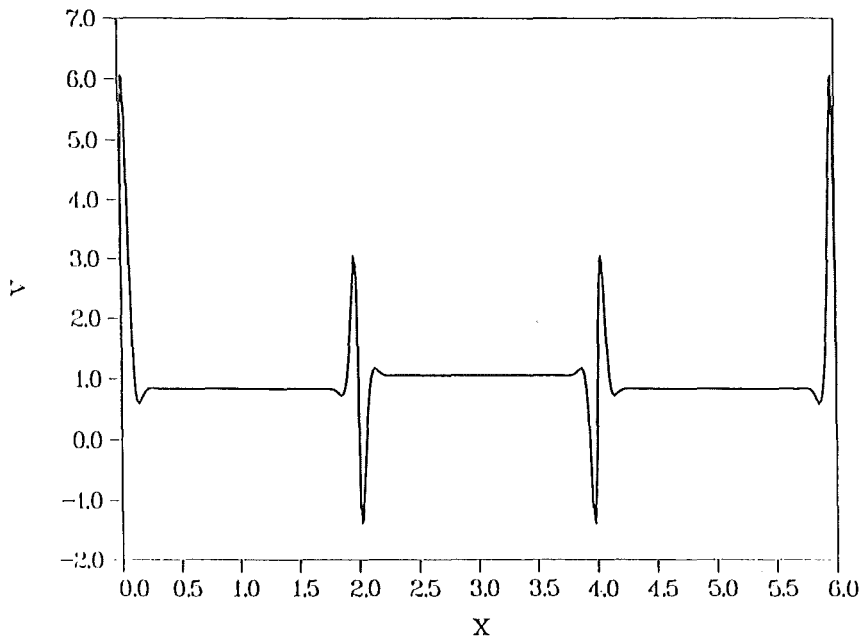


Fig. 8. Fluid velocity in a duct divided into three channels ($n=3$; fixed flow rates) at $y=0$. Here $c_t^{(1)}=c_t^{(3)}=c_s^{(1)}=0.2$; $c_t^{(2)}=c_s^{(2)}=0.1$; $d^{(i)}=2$ for all i ; $M=1000$.

The electric current in the outside side walls is proportional to the induced magnetic field at the wall while in the dividing walls it is proportional to a jump in induced field across the wall (see equations 2.3). Thus a dividing wall acts like a better conductor than an outside side wall, even if their wall conductance ratios are equal. For equal top wall conductance ratios this means that volume flux carried by the layers at the dividing walls is smaller in magnitude than that at the outside side walls.

Variation of the pressure gradients with the side-wall conductance ratio c_s (the same for all side walls) and the Hartmann number is shown on Fig. 9 and 10, respectively. The effect of the finite Hartmann number is to provide an additional path for the electric currents along the side layers and therefore to increase pressure drop. As $M \rightarrow \infty$, pressure gradients tend to finite values given by CFA (see equations 4.2a, 4.5 and 4.6), which is in 5 per cent accuracy with exact values for $c=0.1$ and $M \geq 1000$ (see Fig.10).

CFA overestimates volume flux carried by the side layers. Thus, in situations where side layers play minor role, i.e. carry less volume flux, it should give better results. From Fig. 10 it follows that the best results CFA gives for the middle channel in a three-channel duct, where the flow is almost of Hartmann type. Therefore, in a fully developed multiple duct flow the range of validity of the CFA is wider than in a single-duct flow.

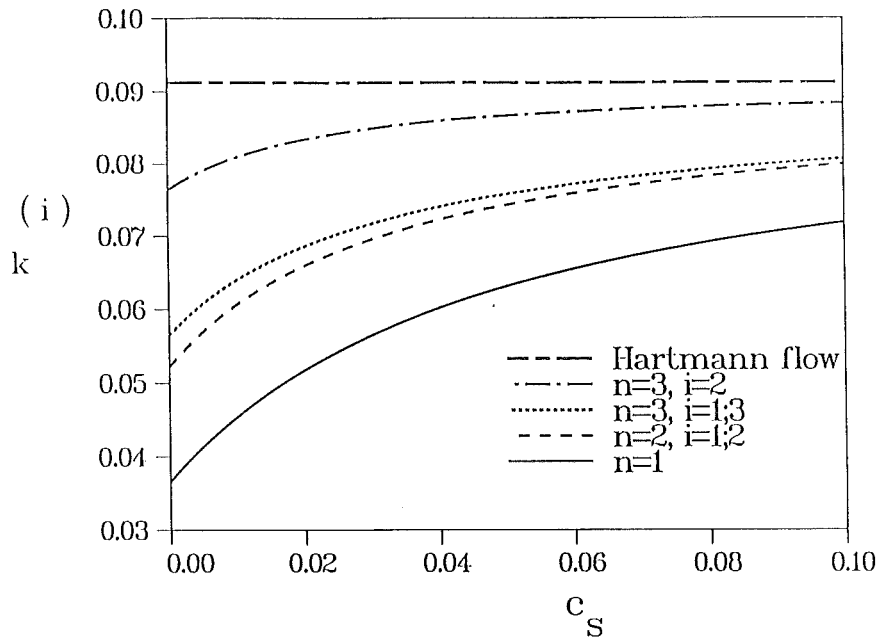


Fig. 9 Variation of pressure gradients with side-wall conductance ratio for $n=1\div 3$. Here $c_t^{(i)}=0.1$; $d^{(i)}=2$ ($i=1\div n$); $M=3000$.

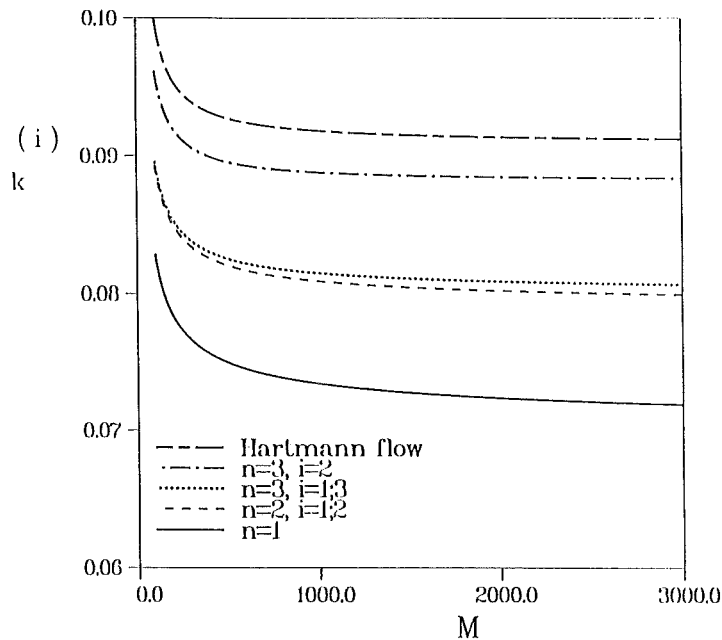


Fig. 10. Variation of pressure gradients with the Hartmann number for $n=1\div 3$. Here $c_t^{(i)}=c_t^{(i)}=0.1$; $d^{(i)}=2$ for all i .

T A B L E 1 VARIATION OF PRESSURE GRADIENTS WITH CHANNEL
NUMBER FOR EQUAL FLOW RATES ($c=0.1, M=3000$).

No. of channels	Pressure gradients $k^{(i)} * 10^2$					
	$i=1$	2	3	4	5	6
1	7.194					
2	7.997					
3	8.070	8.838				
4	8.076	8.913				
5	8.077	8.919	8.987			
6	8.077	8.920	8.994			
7	8.077	8.920	8.994	9.000		

If number of channels is more than three, the flow features remain the same as for $n=3$. Variation of the pressure gradients with channel number is given in Table 1. Pressure gradients in ducts close to the center very soon reach the value $k=0.09$. The latter may be calculated by formula

$$k_{\text{HART}} = (c_t + M^{-1}) / (1 + c_t). \quad (4.9)$$

Therefore, the upper limit for the increase in pressure gradients with respect to the flow in a single duct is given by the ratio of

expressions (4.9) and (4.1b). For wall conductance ratio in the range 0.02+0.4 and Hartmann number in the range 3000+4000 pressure gradients do not increase by more than 30 per cent.

5. CONCLUSIONS

The pressure drop due to MCE in a fully developed flow is found to be not high. The maximum value of the pressure gradient is given by the expression (4.9), which is reached when the channel number exceeds 7. If top wall conductance ratios in all ducts are equal, this value is reached in the ducts close to the center because jets at the dividing walls carrying part of a volume flux disappear.

For the effective cooling of the blanket first wall one would prefer to have equal flow rates in coolant ducts with minimum pressure losses. Therefore, the case of equal both flow rates and pressure gradients seems to be optimal. The analysis for the three-channel duct shows that this can be achieved simply by relating side- and top- wall conductance ratios (see expression 4.8). The same conclusion applies for ducts with more than three channels. To achieve optimal flow distribution the top wall conductance ratios of all channels, except the outer ones, should be made equal first. Then the formula (4.8) applies for the first and the second channels with $\Gamma=0$.

To make the final conclusion about the importance of MCE in the concept of self-cooled liquid-metal blanket one has to analyse the pressure drop in multi-channel bends. It will be addressed in another paper.

REFERENCES

- [1] Malang S., et. al. 1988 Self-cooled liquid-metal blanket concept, *Fusion Technology*, vol. 14, 1343.

- [2] Madarame H., Taghavi K. & Tillack M.S. 1985 The influence of leakage currents on MHD pressure drop, *Fusion Technology*, vol.8, 264.

- [3] John H., Malang S. & Sebening H. (Eds.), 1991 Status report. KfK contribution to the development of DEMO-relevant test blankets for NET/ITER. Part 1: Self cooled liquid metal breeder blanket. Vol. 2: Detailed version. *KfK-4908* (Dezember 1991).

- [4] McCarthy K.A., & Abdou M.A., 1990 Analysis of liquid metal MHD flow in multiple adjacent ducts using an iterative method to solve the core flow equations, *Fusion Engineering and design*, vol. 13, 363.

- [5] Hua T.Q., Walker J.S., Picologlou B.F. & Reed C.B. 1988 Three-dimensional magnetohydrodynamic flows in rectangular ducts of liquid-metal-cooled blankets, *Fusion Technology*, vol. 14, 1389.

- [6] Hua T.Q. & Picologlou B.F. 1991 Magnetohydrodynamic flow in a manifold and multiple rectangular coolant ducts of self-cooled blankets, *Fusion Technology*, vol. 19, 102.

- [7] McCarthy K.A., Ying A.Y., Morley N.B., & Abdou M.A. 1991
Comparison of the core flow approximation and full solution
approach for MHD flow in non-symmetric and multiple adjacent ducts,
Fusion Engineering and Design, vol. 17, 209.
- [8] Temperley D.J., & Todd L. 1971 The effects of wall conductivity
in magnetohydrodynamic duct flow at high Hartmann numbers, *Proc.
Camb. Phil. Soc.*, vol.69, 337.
- [9] Walker J.S. 1981 Magnetohydrodynamic flows in rectangular
ducts with thin conducting walls, *Journal de Mécanique*, vol.20,
No.1, 79.
- [10] Shercliff J.A. 1965 *A textbook of magnetohydrodynamics* (Longmans).
- [11] Shercliff J.A. 1956 The flow of conducting fluids in circular
pipes under transverse magnetic fields, *J. Fluid Mech.*, vol. 1, 644.
- [12] Tabeling P. 1982 Magnetohydrodynamic flows in rectilinear
ducts of rectangular cross-section: the question of the corners,
Journal de Mécanique théorique et appliquée, vol.1, No. 1, 25.
- [13] Cook L.P., Ludford G.S.S. & Walker J.S. 1972 Corner regions in
the asymptotic solution of $\epsilon \nabla^2 u = \partial u / \partial y$ with reference to MHD duct
flow, *Proc. Camb. Phil. Soc.*, vol.72, 117.

- [14] Moon T.J. & Walker J.S. 1990 Liquid metal flow through a sharp elbow in the plane of a strong magnetic field, *J. Fluid Mech.*, vol. 213, 397.
- [15] Hunt J.C.R. 1965 Magnetohydrodynamic flow in rectangular ducts, *J. Fluid Mech.*, vol.21, 577.

APPENDIX A: HARTMANN LAYER HS

The problem governing the flow in the Hartmann layer at the wall i in channel i is

$$\frac{\partial^2 v_{HS}^{(i)}}{\partial y_H^2} + \frac{\partial w_{HS}^{(i)}}{\partial y_H} = 0, \quad \frac{\partial^2 w_{HS}^{(i)}}{\partial y_H^2} + \frac{\partial v_{HS}^{(i)}}{\partial y_H} = 0, \quad (\text{Aa, b})$$

$$v_{HS}^{(i)} = 0, \quad c_t^{(i)M} \frac{\partial w_{HS}^{(i)}}{\partial y_H} = -w_{HS}^{(i)} + k^{(i)} c_t^{(i)M} \quad \text{at } y_H = 0, \quad (\text{Ac, d})$$

$$v_{HS}^{(i)} \Rightarrow v_{SL}^{(i)}(\xi_i, 1), \quad w_{HS}^{(i)} \Rightarrow b_{SL}^{(i)}(\xi_i, 1) - b_C^{(i)} \quad \text{as } y_H \rightarrow -\infty, \quad (\text{Ae, f})$$

where $w_{HS}^{(i)} = b_{HS}^{(i)} - b_C^{(i)}$.

The solution to the problem (Aa-f) is

$$v_{HS}^{(i)} = v_{SL}^{(i)}(\xi_i, 1) \left[1 - \exp(y_H) \right], \quad (\text{Ag})$$

$$w_{HS}^{(i)} = v_{SL}^{(i)}(\xi_i, 1) \exp(y_H) + b_{SL}^{(i)}(\xi_i, 1) - k^{(i)M}. \quad (\text{Ah})$$

Substituting (Ag) and (Ah) into the condition (Ad) gives the relation between functions $v_{SL}^{(i)}(\xi_i, 1)$ and $b_{SL}^{(i)}(\xi_i, 1)$ and hence the boundary condition for side layer variables at $y=1$, namely

$$v_{SL}^{(i)}(\xi_i, 1) \left[c_t^{(i)M} + 1 \right] = -b_{SL}^{(i)}(\xi_i, 1) + k^{(i)M} \left[1 + c_t^{(i)} \right]. \quad (\text{Ai})$$